JOURNAL OF GEOPHYSICAL RESEARCH, VOL. 85, NO. C4, PAGES 1917–1924, APRIL 20, 1980

The Scaling of Vertical Temperature Gradient Spectra

D. R. CALDWELL, T. M. DILLON, J. M. BRUBAKER,
P. A. NEWBERGER, AND C. A. PAULSON

School of Oceanography, Oregon State University, Corvallis, Oregon 97331

Tests of a formula derived for the cutoff wave number of vertical temperature gradient spectra, using data taken in the upper layers of the North Pacific, show encouraging results. To derive this formula, the cutoff wave number is assumed to be the Batchelor wave number, with kinetic energy dissipation calculated by combining a form used in the atmosphere for calculating the vertical eddy diffusivity in terms of the dissipation with the Osborn-Cox formula for calculating eddy diffusivity from the variance of the temperature gradient spectrum. Kinetic energy dissipation in the water column can be determined in this way; a vertical profile of dissipation shows values of the order of 10^{-3} cm^2 s^{-3} at the base of a storm-tossed mixing layer. In the thermocline below, dissipation occurs in patches.

1. INTRODUCTION

Measurements of small-scale temperature gradients from freely falling instruments, a technique pioneered by C. S. Cox [*Gregg and Cox,* 1971], have been performed in a number of locations in the ocean by various investigators [e.g., *Osborn and Cox,* 1972; *Gregg et al.,* 1973; *Gregg,* 1975, 1976, 1977*a*, 1977*b*; *Elliott and Oakey,* 1975, 1976; *Caldwell,* 1976, 1978; *Marmorino and Caldwell,* 1978a, 1978*b*; *Caldwell et al.,* 1978; *Dillon and Caldwell,* 1978]. Interpreting these data has been difficult because of doubt as to whether the full variance of the gradients has been correctly resolved and also because of the lack of an accepted paradigm for the interpretation. The universal turbulence scaling proposed by *Batchelor* [1959] for unstratified flows has been a tempting model, but it has never been shown that this scaling is appropriate in the ocean, which is usually stratified and which is subject to other complicating influences such as surface and internal wave fields.

Confirmation of the Batchelor prediction has been looked for with some success in the laboratory [*Gibson and Schwarz,* 1963] and in a tidal flow [*Grant et al.,* 1968]. In each of these experiments, problems with resolution or noise at the high-frequency end of the spectrum prevented full resolution of the diffusive subrange. In the atmosphere the diffusive limit has been resolved [*Gibson et al.,* 1970; *Williams and Paulson,* 1977], but there the spectral form is quite different from its form in the ocean because of the lower Prandtl number of air.

One attempt to match temperature spectra from a towed body with the Batchelor form failed [*Nasmyth,* 1970], probably because of the procedure followed, which was to force a fit at wave numbers well below the cutoff and then look for coincidence at high wave numbers. The difficulty may lie in the lower reliability of the low wave number points in the usual spectral band-averaging scheme or in the assumption that all of the signal at these frequencies represents turbulence. *Gibson et al.* [1974] suggested the use of a number of features of the universal form in interpreting records from a towed body and found resemblance to the Batchelor form in their spectra [*Gibson et al.,* 1974, Figure 5].

The most recent analyses of vertical temperature gradient spectra are those of *Gregg* [1977*b*] and *Elliott and Oakey* [1976]. *Elliott and Oakey* [1976] chose as a model for their data analysis a series of temperature steps, each spreading by diffusion. This assumption led them to a dependence of energy on the vertical wave number k as exp $(-k^2)$, the same dependence as that in the cutoff of the Batchelor form. They take the mean time since step formation, $\bar{t}$, as an adjustable parameter found for each set of data. If the assumption is made that their spectra follow the Batchelor form, values of kinetic energy dissipation ϵ can be calculated from their values of $\bar{t}$($\epsilon = \nu\bar{t}^{-2}$, where ν is the kinematic viscosity). Values of ϵ calculated in this manner range, quite reasonably, from 2×10^{-5} to 5×10^{-4} cm^2 s^{-3} for various casts. Thus there is nothing in their results inconsistent with an interpretation in terms of the Batchelor spectrum.

Gregg's conceptual picture is of a spectrum composed of (1) the signature of internal waves and 'fine structure' which dominates at low wave numbers (<0.02 cycles cm^{-1}) and (2) 'microstructure' at higher wave numbers, the source of which is uncertain. Figure 18 of *Gregg*'s [1977*b*] paper illustrates this idea, and an analysis based on it shows a high wave number peak similar to the Batchelor spectrum [*Gregg,* 1977*b*, Figure 16], although he does not choose to interpret it so. In the present work we use his concepts for interpreting the spectra, but we treat the data somewhat differently and attempt to test quantitatively the hypothesis that Batchelor scaling describes vertical temperature gradient spectra for the highest wave numbers.

We propose a scaling of the wave number k_c at which the energy in the spectrum has decreased to 12% of its value in the microstructure peak and use data obtained by dropping a freely falling instrument through surface layer, thermocline, and halocline in the North Pacific to test this scaling. We chose 12% because the Batchelor spectrum falls to this percentage of its peak value at the Batchelor wave number if $q = 2.2$ [*Williams and Paulson,* 1977].

In a companion paper [*Dillon and Caldwell,* 1980] the hypothesis that the shape of the vertical temperature gradient is similar to that of the Batchelor spectrum is examined. The reader should refer to it for more experimental detail and more discussion of the form and parameters of the spectrum.

2. THE PROPOSED SCALING

Lilly et al. [1974] and *Weinstock* [1978] proposed for vertical eddy diffusivity in stably stratified flows a relation which, in Weinstock's form, is

$$K_z = 0.8\epsilon/N^2 \qquad (1)$$

where N is the buoyancy frequency and K_z is a vertical eddy diffusivity. If we combine this with the *Osborn and Cox* [1972]

Paper number 9C1647.
0148-0227/80/009C-1647$01.00

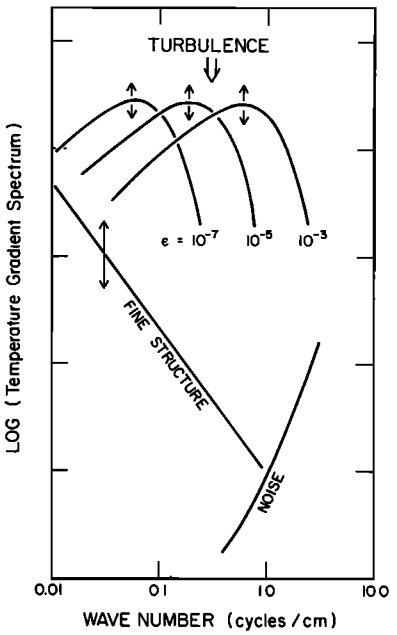

Fig. 1. Schematic of interpretation of spectra. The 'Fine structure' contribution has been plotted as $k^{-3/2}$. Both k dependence and level vary widely. The 'turbulence' contribution is placed in wave number by the value of ϵ, but its position vertically on this plot depends on mean gradient and Cox number as well. The 'noise' contribution is shown as modified by the thermistor response correction. Its position varies with drop speed only.

formula for obtaining eddy diffusivities from vertical temperature gradient data,

$$K_z = D \cdot Cx \tag{2}$$

where $Cx \equiv \langle (dT/dz)^2 \rangle / \langle dT/dz \rangle^2$ is the Cox number and D is the thermal diffusivity, we can solve for ϵ to obtain

$$\epsilon = (1/0.8) N^2 D Cx \tag{3}$$

All quantities on the right-hand side are available to us from vertical temperature and conductivity profiles if the variance of dT/dz is completely resolved. If next we insert this expression for ϵ in the formula for the Batchelor wave number (wave numbers are herein defined as the reciprocals of wavelengths), we obtain

$$k_B \equiv \frac{1}{2\pi}\left(\frac{\epsilon}{\nu D^2}\right)^{1/4} = \frac{1}{2\pi}\left(\frac{N^2 Cx}{0.8 \nu D}\right)^{1/4} \tag{4}$$

The hypothesis that we shall test is that the experimentally determined values of the cutoff wave number k_c are related to this formulation of k_B; conceivably, the two might be identical.

3. The Data

The freely falling instrument used was similar to one previously described [*Caldwell et al.*, 1975]. Slowed by helicopter-type wings, it descends at a speed adjustable from 5 to 25 cm s^{-1}. Signals from thermistors in the nose (bottom) of the instrument and from a pressure sensor are transmitted through a data link to the ship and are processed and recorded on digital magnetic tape with a 45-Hz Nyquist frequency. The records used to compute temperature gradient spectra were processed by a 12-pole Butterworth low-pass filter with a 30-Hz 3-dB point and were time-differentiated before digitizing and recording. Frequency spectra were calculated, corrected for thermistor and electronics transfer functions, and then translated to vertical wave number spectra by use of the drop speed determined from the pressure sensor record.

A conductivity sensor (Neil Brown), also mounted on the nose of the instrument, was used to derive salinities, densities, and buoyancy frequencies, especially in the halocline.

Let us consider what we expect to be able to see with such an instrument as it falls through the water column. Fall speeds must be slow enough to allow the temperature sensor to respond to the very thinnest temperature gradient to resolve fully the temperature gradient spectrum. For the data to be used in this paper the fall rate was 10 cm s^{-1}, and the 3-dB frequency response of the thermistors was about 7 Hz so that in terms of vertical wave numbers the 3-dB point is 0.7 cycles/cm^{-}. According to the Batchelor model, the value of ϵ corresponding to a cutoff wave number of 0.7 cycles cm^{-1} is approximately 2×10^{-5} cm^2 s^{-3}. Therefore to resolve spectra extending to the Batchelor wave number, the data must be corrected for transducer response if ϵ is larger than 2×10^{-5}

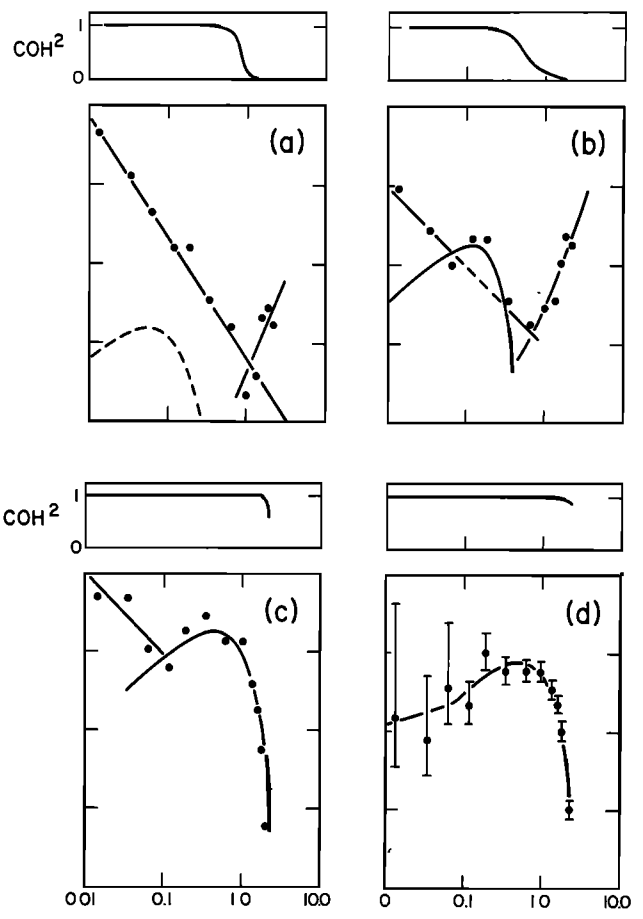

Fig. 2. Examples of observed spectra. Here 512 points at 90 points per second are used, Gaussian windowed. Two signals from the thermistor are amplified and recorded separately, so the coherence between them, shown above each spectrum, discriminates signal from noise (because the noise source lies mainly in the amplifiers). All data were recorded on August 23 in 18 m s^{-1} winds: (*a*) 51-m depth, turbulence level so low that fine structure dominates, noise shows up at right; (*b*) 54-m depth, all three components at comparable levels, turbulence just visible; (*c*) 40-m depth, turbulence signal dominates noise, fine structure just visible at left; (*d*) 32-m depth, only the turbulence signal is visible. The 95% confidence limits in Figure 2*d* apply to Figures 2*a*–2*c* also.

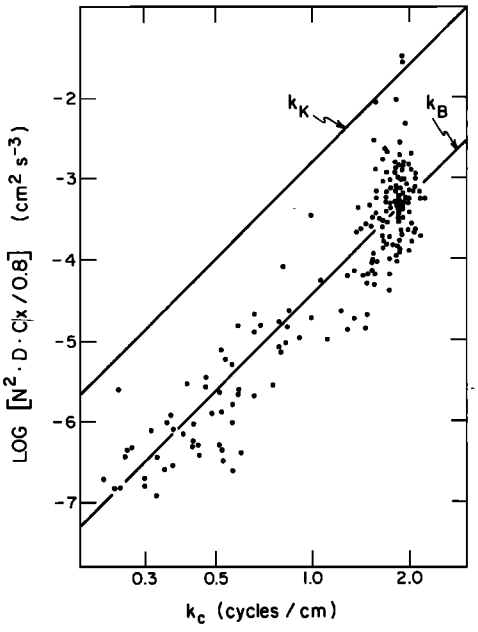

Fig. 3. Kinetic energy dissipation calculated as prescribed versus wave number k_c at which the spectrum has fallen to 12% of its peak value. The points come from the lower mixed layer and the thermocline on one cast on August 23, 1977. Lines are drawn to represent the Kolmogorov (k_k) and Batchelor (k_B) wave numbers.

$cm^2\ s^{-3}$. Since the signals are low passed at 30 Hz before recording to suppress 60-Hz interference, the highest wave number accessible to us at the 10 cm s^{-1} descent rate is 3 cycles cm^{-1}, corresponding to an energy dissipation of 3.5×10^{-3} $cm^2\ s^{-3}$. A lower bound on the wave numbers at which the turbulence signal can be seen is set by the background spectrum due to other causes, which dominates at low frequency. This varies, but the lowest resolvable value of ϵ is often approximately 10^{-7} $cm^2\ s^{-3}$ in the thermocline. The situation is therefore that the signal at the Batchelor wave number, if present can be seen in these records for $10^{-7} < \epsilon < 2 \times 10^{-5}$ $cm^2\ s^{-3}$ with no corrections for thermistor response and to 3.5×10^{-3} $cm^2\ s^{-3}$ with correction.

Because the fluctuations encountered by the instrument as it descends are often seen by the thermistor as being near the highest frequencies that it can resolve, it must be established that the cutoffs seen in the spectra represent the high wave number limit of fluctuations present in the water column

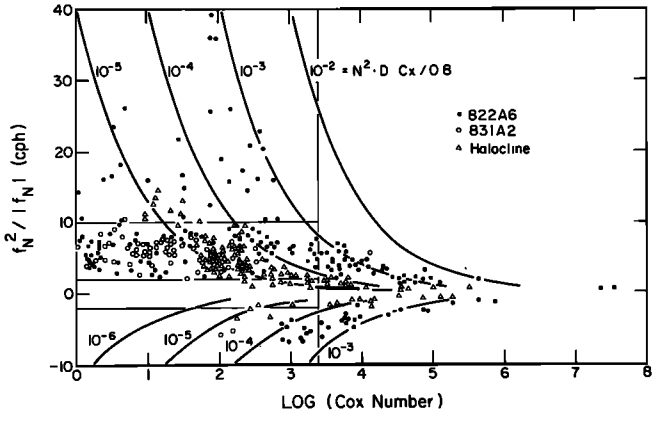

Fig. 4. Loci of all data used, in (f_N, Cx) space. The vertical scale is chosen to be linear in f_N, imaginary values of f_N appearing as negative numbers.

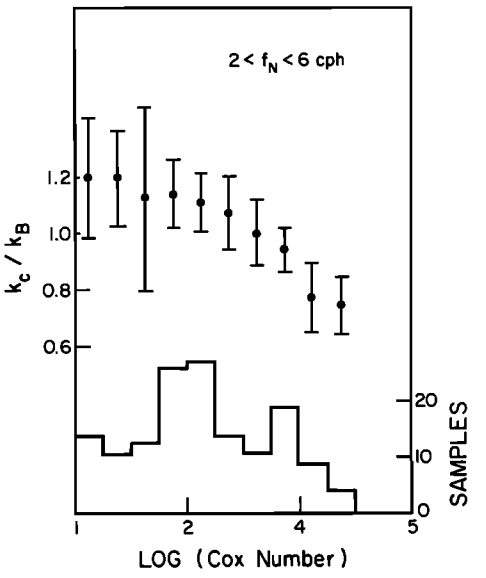

Fig. 5. Ratio of observed cutoff wave number to Batchelor wavenumber versus Cox number for $2 < f_N < 6$ cph. The number of samples averaged into each band is given. The error bars shown are 95% confidence limits.

rather than being caused by some instrumental effect. The reader is referred to the companion paper [*Dillon and Caldwell*, 1980] for a more detailed discussion of the shapes of these spectra and the method used to determine them, in particular for a description of the determination of the thermistor's frequency response correction. Without repeating the details given there we can list three reasons why this cutoff must be a property of the water column:

1. The correction used for frequency response, originally determined by comparison of data from a thermistor of the

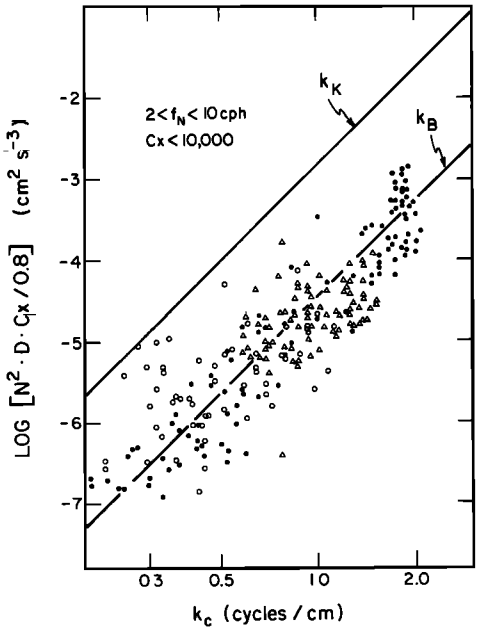

Fig. 6. Dissipation calculated as prescribed versus cutoff wave number. Cases with Cox number less than 10^4 and f_N between 2 and 10 cph are included. The data are those of Figure 4 (solid circles), together with data from the mixed layer on September 1 in 14 m s^{-1} winds (triangles) and data from various casts through the halocline (open circles). Lines are drawn to represent the Kolmogorov (k_k) and Batchelor (k_B) wave numbers.

TABLE 1. Results of Applying Regression Models of the Form $10^a f_N{}^b Cx^c$ to Cases for Which $f_N > 2$ cph, $Cx < 2500$

Model	a	b	c	E^2	F_3	F_1
1	−0.971	0.50	0.25	0.0188	38	
2	−0.92 ± 0.07	0.50	0.25	0.0164	3	−31
3	−0.97 ± 0.07	0.57 ± 0.07	0.25 ± 0.02	0.0162		
4	−0.47 ± 0.05	0.00	0.22 ± 0.03	0.0349	276	
5	−0.44 ± 0.11	0.43 ± 0.13	0.00	0.0609	659	
6	−0.98 ± 0.05	0.57 ± 0.07	0.25	0.0161	−1	
7	−0.91 ± 0.03	0.50	0.24 ± 0.02	0.0164	3	

*Values of a, b, and c with error limits are determined form the data. Other values of a, b, and c are assumed. The errors given are 95% confidence limits. E^2 is the mean square deviation relative to each model, F_3 is the standard statistical parameter F calculated for each model relative to model 3, and F_1 is the value of F relative to Model 1. A value of F of 3 or greater corresponds to a chance of less than 1% that the mdoels are not significantly different; 242 samples are included, 68% of the total data set.

same model with data obtained simultaneously from a thermocouple with much faster response, is described in the appendix. A redetermination in the laboratory [*Dillon and Caldwell,* 1980] confirmed this correction with the required errors (see discussion below). A slightly different test performed by M. C. Gregg (personal communication, 1979) gave similar results. Therefore considerable confidence can now be placed in the correction.

2. In many of the determinations of the cutoff wave number the frequencies were well below those at which any correction is required according to these tests, and no systematic difference was seen between these and higher-frequency data.

3. The effect of the estimated error in this correction on the hypothesis test made in this paper is not significant, as is shown in the appendix. Even a much larger error would not change the conclusions.

These data were obtained on the mixed layer experiment (Mile) cruise in August 1977 at 50°N, 145°W (ocean station P) on board the R/V *Oceanographer.* For the present work only a few of the 381 microstructure profiles obtained are considered. One cast (822A6) through surface layer and thermocline during 18 m s^{-1} winds, one cast through the surface layer in lighter (14 m s^{-1}) winds in a latter storm (831A2), and a collection of data taken at various times in the halocline at 100–130 m are used. Thus the hydrographic regions sampled include active mixing layers at several wind speeds, the thermocline (35–62 m), and a temperature inversion well stabilized by its salt gradient.

4. PROCEDURE

Spectra were calculated for record segments spanning approximately 60 cm in the vertical, comprising 512 points recorded at the rate of 90 s^{-1}. A Gaussian window was applied to each segment before the Fourier transform was performed. Such thin sections were used to make certain that conditions would not change too much within the segment, particularly the buoyancy frequency and the dissipation. In our interpretation the observed spectra result from the superposition of three separate components: fine structure, turbulence, and noise (Figure 1). We imagine the fine structure component to be due to the basic shape of the temperature profile, the straining of the temperature profile by internal waves, and the remnants of mixing events of medium scale. As judged from the spectra that it dominates, the spectral values usually fall as (wave number)$^{-n}$, with n in the range −1 to −2. It dominates in parts of the thermocline where stratification is strong and turbulence is weak (Figure 2*a*). The noise spectrum has the form (frequency)$^{-1}$ before differentiation of the signal and correction for thermistor response; after differentiation, correction, and translation to wave number it increases with wave number as $k \cdot [1 + (S_D k/f_1)^2]$, where s_D is the drop speed and f_1 the 3-dB frequency of the correction filter. Noise dominates only in the upper part of the mixed layer where temperature signals are very small because of the lack of stratification. Discrimination between signal and noise is made by examining the coherence between signals originating in the same thermistor but amplified separately. The source of the noise lies mainly in the amplifier, so coherence is lost when noise dominates (Figure 2*b*).

The Batchelor spectrum (Figure 2*d*) has a shape completely specified once the values of the 'universal' and molecular constants are set, but its vertical position on the plot depends on the Cox number and the mean gradient, and its position in wave number depends on the kinetic energy dissipation.

Depending on the relative power in these components of a particular observed spectrum, it may or may not be possible to detect the turbulence component. If one can be seen, the cutoff wave number k_c (operationally defined as the wave number at which the power density in the turbulence component falls to 12% of its peak value) and the Cox number can be calculated. In these calculations, care must be taken that only the turbulence signal is used.

TABLE 2. Results of Models for $2 < f_N < 10$ cph, $Cx < 2500$

Model	a	b	c	E^2	F_3
1	−0.971	0.50	0.25	0.0181	19
2	−0.93 ± 0.10	0.50	0.25	0.0165	−1
3	−0.97 ± 0.10	0.56 ± 0.12	0.25 ± 0.02	0.0165	
4	−0.53 ± 0.05	0.00	0.23 ± 0.02	0.0243	93
5	−0.32 ± 0.16	0.25 ± 0.22	0.00	0.0623	550
6	−0.97 ± 0.08	0.56 ± 0.11	0.25	0.0165	−1
7	−0.92 ± 0.04	0.50	0.25 ± 0.02	0.0165	0

Sample includes 202 cases, 57% of total. Values of a, b, and c with error limits are determined from the data. Other values of a, b and c are assumed.

TABLE 3. Results of Regression Models for All f_N, With $Cx > 2500$

Model	a	b	c	E^2	F_3	M
1	−0.971	0.50	0.25	0.0466	161	
2	−1.11 ± 0.24	0.50	0.25	0.0269	58	
3	−0.92 ± 0.22	0.72 ± 0.10	0.19 ± 0.04	0.0158		0.83
4	−0.07 ± 0.26	0.00	0.01 ± 0.06	0.0505	181	0.04
5	−0.03 ± 0.05	0.45 ± 0.12	0.00	0.0296	72	0.64
6	−1.21 ± 0.04	0.81 ± 0.09	0.25	0.0172	7	0.89
7	−0.62 ± 0.16	0.50	0.13 ± 0.04	0.0190	16	0.61

Sample includes 86 cases, 24% of the total. M is the multiple regression coefficient. Values of a, b, and c with error limits are determined from the data. Other values of a, b, and c are assumed.

The definition of Cox number given in section 2 on the proposed scaling is appropriate to a completely stratified situation in which horizontal gradients are negligible. For isotropic gradients these Cox numbers should be multiplied by 3. In the following discussion we shall not use the factor of 3, but bear in mind that these values may be lower than they should be.

The buoyancy frequency N and its equivalent in cycles per hour, f_N, are calculated for the same segment of data. The TS relation was found to hold so well in the surface layer over this period, and the saline component of the density gradient was so small, that N was calculated from the vertical temperature gradient with a linear correction for salinity. In the halocline, data from the conductivity cell had to be used, because the salinity completely dominates the density structure there.

5. Results

If all the assumptions and approximations implicit in the derivation in section 2 have not led us astray, a plot of k_c versus $0.8^{-1}N^2 \cdot D \cdot Cx$ for many spectra should make sense, and indeed it does for all the data from one cast (Figure 3). The points cluster about the line representing (4) very nicely, even though both stable and unstable segments have been included, and the Cox number ranges from values as small as 1.05, where turbulence is so small that diffusion is almost precisely molecular, to values as large as 10^7, where stratification is nearly absent. Any possibility of circularity in this scaling is ruled out by the observation that molecular viscosity is included in the computation of the Batchelor scale and nowhere else.

To further investigate this scaling under varying conditions, all the cases available in the halocline (62) are added to the data set along with 113 cases from the mixed layer during milder (14 m s^{-1}) winds. The distribution in (N, Cx) space is not uniform (Figure 4). Large Cox numbers are never seen in regions with large N, and small N is never combined with small Cox number. Examination of the ratio k_c/k_B averaged over regions in this plot reveal (1) a systematic trend to low values of k_c/k_B at large Cox numbers (Figure 5), (2) a trend to low values at small N, (3) some trend to larger values for very large N, and (4) no difference between stable and unstable cases at similar values of N. Values of k_c/k_B most consistently near 1 are found in the region $Cx < 2500$, $2 < f_N < 10$ cph, in which 57% of the points are located. By replotting ϵ versus k_c for these cases an even more consistent picture is seen (Figure 6).

To examine this scaling further, and in particular to find out if the inclusion of N is justified, a number of multiple regression analyses were performed on subsets of these 354 samples. A series of models was used, based on $k_c = 10^a|f_N|^b(Cx)^c$, expressed for analysis as

$$\log_{10} k_c = a + b \log_{10} |f_N| + c \log_{10} (Cx) \qquad (5)$$

to emphasize deviations properly as being fractional rather than absolute. Here f_N is the buoyancy frequency expressed in cycles per hour. To see which parameters were significant, various combinations of fixed and fitted parameters were used (Table 1). These models are (1) equation (4), (2) equation (4) with the constant given as 1/0.8 allowed to be determined by the data, (3) equation (5) with a, b, and c determined by the data, (4) same as (3) but with no f_N dependence, (5) same as (3) but with no Cox number dependence, (6) c set to $\frac{1}{4}$ and a and b determined by the data, and (7) $b = \frac{1}{2}$ and a and c determined by the data. Results are as follows.

1. For stable stratification and moderate Cox numbers (when f_N is larger than 2 cph and the Cox number is less than 2500) the F test shows that models 2, 3, 6, and 7 cannot be differentiated on the basis of these data with 95% confidence (Table 1). We therefore conclude that the dependence on f_N and Cx is as $f_N{}^{0.5}Cx^{0.25}$, as hypothesized. Because model 4 fails badly in comparison with model 3, we conclude that the dependence on f_N is required to explain these data. By comparing model 2 with model 1 it might be concluded that the

TABLE 4. Results of Regression Models for $f_N < 2$ cph, $Cx < 2500$

Model	a	b	c	E^2	F_3	M
1	−0.971	0.50	0.25	0.010	0.0	
2	−0.96 ± 0.36	0.50	0.25	0.010	0.6	
3	−1.12 ± 0.34	0.46 ± 0.34	0.32 ± 0.09	0.010		0.91
4	−0.81 ± 0.30	0.00	0.33 ± 0.10	0.015	5.7	0.85
5	−0.27 ± 0.52	0.49 ± 0.74	0.00	0.049	48.5	0.33
6	−0.93 ± 0.25	0.46 ± 0.36	0.25	0.0106	1.5	0.57
7	−1.15 ± 0.24	0.50	0.32 ± 0.08	0.010	−0.9	0.90

Sample includes 16 cases, 4.5% of the total. Values of a, b, and c with error limits are determined from the data. Other values of a, b, and c are assumed.

TABLE 5. Results of Regression Models for $f_N > 10$ cph, $Cx < 2500$

Model	a	b	c	E^2	F_3	M
1	−0.971	0.50	0.25	0.022	20.6	
2	−0.88 ± 0.30	0.50	0.25	0.014	−0.8	
3	−0.73 ± 0.28	0.39 ± 0.24	0.24 ± 0.05	0.014		0.88
4	−0.29 ± 0.10	0.00	0.26 ± 0.05	0.018		0.84
5	−0.66 ± 0.54	0.63 ± 0.44	0.00	0.049	90.7	0.42
6	−0.73 ± 0.28	0.38 ± 0.24	0.25	0.014	−0.9	0.46
7	−0.86 ± 0.08	0.50	0.24 ± 0.05	0.014	−0.1	0.85

Samples include 40 cases, 11% of the total. Values of a, b, and c with error limits are determined from the data. Other values of a, b and c are assumed.

constant term 10^a is 12% larger than was assumed. This could mean that the constant given as 0.8 by Weinstock is 12% smaller, 0.71; that the Cox numbers should have been multiplied, on the average, by a factor of 1.6; or that the universal constant q is not 2.2, as we have chosen it [*Dillon and Caldwell*, 1980]. Still more likely, all of these effects are involved, or perhaps the f_N dependence is a bit greater than is predicted (compare 1 versus 3).

2. For stable but not large stratification and moderate Cox numbers ($2 < f_N < 10$ cph, $Cx < 2500$) the result is the same as result 1 but with points in the steepest part of the thermocline rejected. Again, models 2, 3, 6, and 7 are indistinguishable, showing that with these data, model 2 cannot be rejected (Table 2). Again, the constant term is larger, by 10% this time. A comparison of models 3 and 4 shows that even for this restricted range in f_N the inclusion of f_N is justified.

3. For large Cox numbers ($Cx > 2500$), regardless of stability the results deviate from the models that work so well for smaller Cox numbers (Table 3). Perhaps the multiple regression coefficients are the most illuminating statistic, particularly in the comparison of model 4 and 5. Here it is seen that little of the variance can be explained by the Cox number dependence but much more by the f_N dependence. The nature of the sampling makes this even more impressive, the range in f_N being so much more restricted. In general, models 1 and 2 are very poor. We conclude that one or more of our assumptions are violated for large Cox numbers.

4. For unstable stratification, moderate Cox number ($f_N^2/|f_N| < -2$ cph, $Cx < 2500$), few cases were found (Table 4). The results are consistent with those for stable stratification, but the resolution is very poor.

5. For small stratification and moderate Cox number ($|f|_N < 2$ cph, $Cx < 2500$): too few cases were found to draw any conclusions.

6. Cases with large, stable stratification and moderate Cox number ($f_N > 10$ cph, $Cx < 2500$); also included with less stable points in the data of Table 1, are found only in the steepest part of the thermocline. The regression analyses (Table 5) show that these cases scale consistently with the less stable cases, but again resolution is poor.

7. For all stabilities and moderate Cox numbers ($Cx < 2500$) it must be noted that so many cases have moderate, stable f_N that these dominate. The results show that the f_N dependence may be significantly greater than 0.50 power; this calculation yields 0.60 ± 0.06 for the exponent of f_N (Table 6). Otherwise the scaling works very well. The model 3 results give the exponent of the Cox number as 0.25 ± 0.02 and the constant term as −0.97 ± 0.06, both precisely as in the proposed scaling.

Values of the Cox number and k_c cannot be calculated in every case. In the thermocline the mean stratification—and perhaps also the effects of internal wave straining—may dominate the spectrum, so that the turbulence signal cannot be seen. In the mixed layer, signal levels may be so low that noise interferes. In the 18 m s^{-1} storm in which many of these data were obtained, turbulence near the surface was so intense that the instrument was tipped and the drop speeds were erratic. Even with these difficulties a picture can be made of the dissipation versus depth (Figure 7) by using (3). Here dissipations in the mixed layer are of the order of 10^{-4}–10^{-3}. In the thermocline there are patches of dissipation of the order of 10^{-5}–10^{-4}, but apparently, dissipations in much of the thermocline are considerably lower. It must be kept in mind that some dissipative regions may be invisible to this method because turbulence is seen only as it manifests itself in temperature fluctuations; an isothermal layer gives no signal regardless of its dissipation.

6. DISCUSSION

Now that it has been shown that the Lilly-Weinstock formula for calculating vertical eddy diffusivity from ϵ and N,

TABLE 6. Results of Regression Models for All f_N, $Cx < 2500$

Model	a	b	c	E^2	F_3	M
1	−0.971	0.50	0.25	0.0183	41	
2	−0.93 ± 0.06	0.50	0.25	0.0166	12	
3	−0.97 ± 0.06	0.60 ± 0.06	0.25 ± 0.02	0.0159		0.88
4	−0.45 ± 0.05	0.00	0.20 ± 0.03	0.0398	401	0.66
5						
6	−1.01 ± 0.05	0.60 ± 0.06	0.25	0.0158	−1	0.79
7	−0.91 ± 0.03	0.50	0.24 ± 0.02	0.0165	10	0.86

Sample includes 268 cases, 75% of total. Values of a, b, and c with error limits are determined from the data. Other values of a, b, and c are assumed.

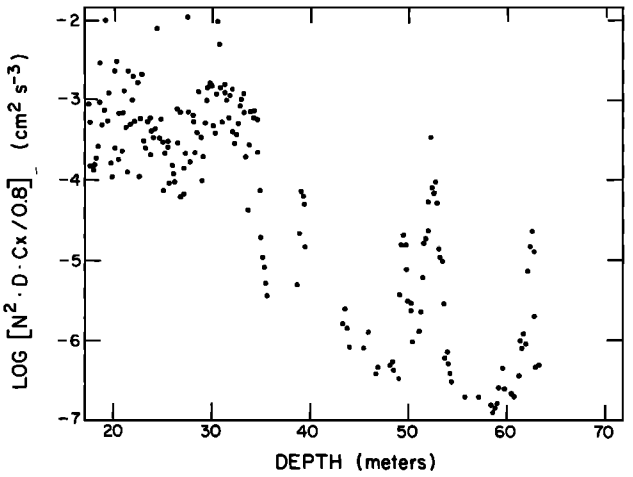

Fig. 7. Dissipation calculated as prescribed versus depth for the cast on August 23, 1977.

the Cox-Osborn formula for calculating eddy diffusivity from temperature gradient measurements, and the Batchelor universal spectral form can be combined to yield a relation between the cutoff wave number and the Cox number and buoyancy frequency (for limited Cox number), are we to conclude that all these relations are correct? Can we now assume that, as long as the Cox number is less than 2500, ϵ can be correctly calculated either from the Cox number and N or from k_c by inverting the formula for the Batchelor wave number? More confirmation is needed, the key information required being measurements of dissipation from microscale shear measurements [e.g., *Osborn,* 1974] made on a vehicle from which simultaneous measurements like those described in this paper are being made.

Why does this scaling for the cutoff wave number, which seems to work so well for conditions of moderate Cox number, fail when the Cox number is large? Additional evidence may be found in the companion paper [*Dillon and Caldwell,* 1980], in which it is shown that the spectrum of the turbulent fluctuations closely resembles the Batchelor form only when the Cox number is large. The failure then is not in the Batchelor spectrum or its assumptions. We suspect that the failure lies in the assumed formula for vertical eddy diffusivity in terms of ϵ and N. This formula cannot be expected to hold in weak stratification, where the turbulence is so strong that the remaining stratification cannot affect it. The observation (Table 3) that cutoff wave number becomes independent of Cox number in this case might mean that an asymptotic state has been reached. The scaling of k_B as we have expressed it still obtains, but the test can no longer validate it. Our hypothesis, which requires a further test, is now that the Batchelor scaling in terms of ϵ governs the high wave number cutoff of the temperature gradient spectrum whether or not the spectrum follows the Batchelor form at lower wave numbers. A method of determining ϵ for high Cox numbers, such as the small-scale shear measurement, is required for the test.

APPENDIX

As is seen above, to observe fluctuations at the Batchelor wave number with a 10 cm s^{-1} drop speed for dissipations greater than 2×10^{-5} cm^2 s^{-3}, the frequency response function for the thermistor must be established for correcting the spectra. Before discussing the response functions used, let us examine in detail the effect on determinations of Cox number

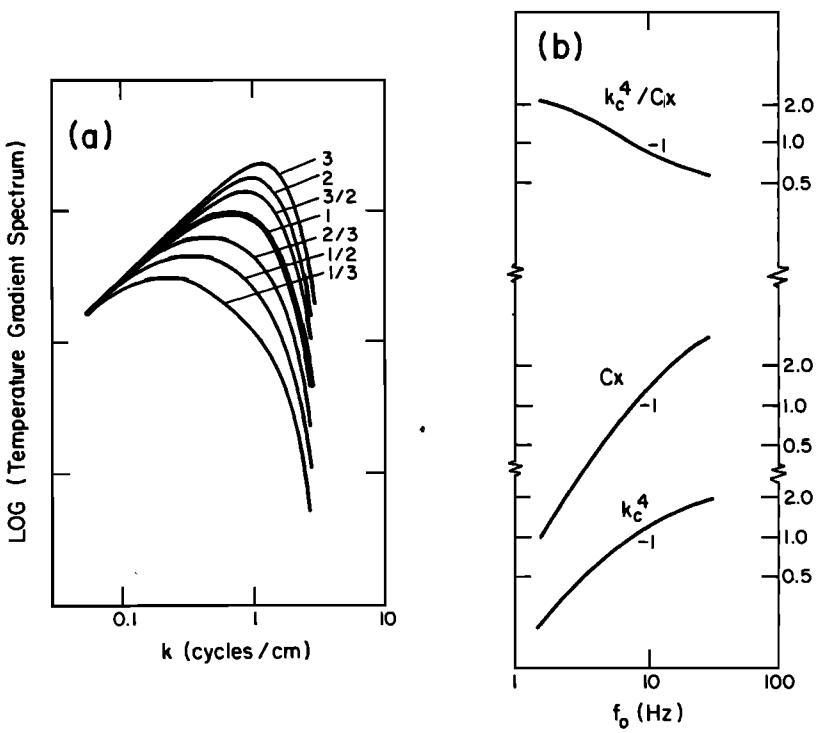

Fig. 8. Effect of erroneous correction for thermistor response. The assumed spectrum (labeled 1) is attenuated by the factor $[1 + (s_D k/f_0)^2]^{-1}$ and then corrected by the factor $[1 + (s_D k/f_1)^2]$, with f_0 assuming various values but f_1 always being 7.4 Hz (s_D is the drop speed in centimeters per second). (*a*) Resultant spectra labeled with the appropriate values of f_0/f_1. (*b*) Ratios of various quantities to their values when $f_0 = f_1$ is plotted versus f_0.

and k_c of errors in the response functions as follows: Assume that a spectrum with the Batchelor form and cutoff at 28 Hz ($\epsilon = 2.5 \times 10^{-3}$ cm^2 s^{-3}) represents the temperature fluctuations in a segment of the water column. Assume also that a thermistor passes through this segment and observes these fluctuations, attenuating the signals at the various frequencies as $[1 + (f/f_0)^2]^{-1}$. Now examine the effect of correcting the spectrum with the factor $[1 + (f/f_1)^2]$ with various values of f_1. Then calculate the Cox number, and measure the cutoff frequency as a function of f_1/f_0, the ratio of assumed and real correction scales in frequency. Results of this numerical experiment (Figure 8) show the effect of various degrees of error in correction on spectra and determined values of k_c and the Cox number. The hypothesis test performed depends on k_c^4/Cx, a quantity which depends little on the correction (Figure 8).

The response function used in the present work was obtained by comparing simultaneous spectra obtained from a thermistor of the type used and from a 0.0025-cm-diameter thermocouple in freshwater. The correction is approximated by $1 + (f/f_1)^2$. At the descent rate of the instrument, 10 cm s^{-1}, f_1 is 7.4 Hz, so the correction is a multiplicative factor of 17.4 at the highest frequency used here, 30 Hz. A redetermination of the response function by passing the thermistor through a thin jet of warm water in a laboratory tank [*Dillon and Caldwell*, 1980] shows that the response is reasonably well described by a value of f_1 of 6.8 Hz, about 8% lower than that indicated by the field experiments. Referring to Figure 8, this discrepancy in f_1 corresponds to a difference in k_c of less than 1% and a change in the ratio $k_c/Cx^{1/4}$ of less than 1%. Similar results for the same type of thermistor are found by M. C. Gregg (private communication, 1979). Thus the corrections used in this paper are sufficiently accurate for the purpose. To examine the detailed form of the spectra, a more complicated response correction is required, such as that in the companion paper.

Acknowledgment. This work has been supported by the Office of Naval Research, contract N0014-76-C-0067.

REFERENCES

Batchelor, G. K., Small scale variation of convected quantities like temperature in turbulent fluid, *J. Fluid Mech. 5,* 113–133, 1959.

Caldwell, D. R., Fine-scale temperature structure in the bottom mixed layer on the Oregon shelf, *Deep Sea Res., 23,* 1025–1036, 1976.

Caldwell, D. R., Variability of the bottom mixed layer on the Oregon shelf, *Deep Sea Res., 25,* 1235–1243, 1978.

Caldwell, D. R., S. Wilcox, and M. Matsler, A relatively simple and inexpensive probe for fine-scale temperature measurements, *Limnol. Oceanogr., 20,* 1035–1042, 1975.

Caldwell, D. R., J. M. Brubaker, and V. T. Neal, Thermal microstructure on a lake slope, *Limnol. Oceanogr., 23,* 372–374, 1978.

Dillon, T. M., and D. R. Caldwell, Catastrophic events in a surface mixed layer, *Nature, 276,* 601–602, 1978.

Dillon, T. M., and D. R. Caldwell, The Batchelor spectrum and dissipation in the upper ocean, *J. Geophys. Res., 85,* this issue, 1980.

Elliott, J. A., and N. S. Oakey, Horizontal coherence of temperature microstructure, *J. Phys. Oceanogr., 5,* 506–515, 1975.

Elliott, J. A., and N. S. Oakey, Spectrum of small-scale oceanic temperature gradients, *J. Fish. Res. Bd. Can., 33,* 2296–2306, 1976.

Gibson, C. H., and W. H. Schwarz, The universal equilibrium spectra of turbulent velocity and scalar fields, *J. Fluid Mech., 16,* 365–384, 1963.

Gibson, C. H., G. R. Stegen, and R. B. Williams, Statistics of the fine structure of turbulent velocity and temperature fields at high Reynolds number, *J. Fluid Mech., 41,* 153–167, 1970.

Gibson, C. H., L. A. Vega, and R. B. Williams, Turbulent diffusion of heat and momentum in the ocean, *Advan. Geophys., 18A,* 353–370, 1974.

Grant, H. L., B. S. Hughes, W. M. Vogel, and A. Moilliet, Some observations of the occurrence of turbulence in and above the thermocline, *J. Fluid Mech., 34,* 443–448, 1968.

Gregg, M. C., Microstructure and intrusions in the California current, *J. Phys. Oceanogr., 5,* 253–278, 1975.

Gregg, M. C., Finestructure and microstructure observations during the passage of a mild storm, *J. Phys. Oceanogr., 6,* 528–555, 1976.

Gregg, M. C., A comparison of finestructure spectra from the main thermocline, *J. Phys. Oceanogr., 7,* 33–40, 1977*a*.

Gregg, M. C., Variations in the intensity of small-scale mixing in the main thermocline, *J. Phys. Oceanogr., 7,* 436–454, 1977*b*.

Gregg, M. C., and C. S. Cox, Measurements of the oceanic microstructure of temperature and electrical conductivity, *Deep Sea Res., 18,* 925–934, 1971.

Gregg, M. C., C. S. Cox, and P. W. Hacker, Vertical microstructure measurements in the central North Pacific, *J. Phys. Oceanogr., 3,* 458–469, 1973.

Lilly, D. K., D. E. Waco, and S. I. Adelfang, Stratospheric mixing estimated from high-altitude turbulence measurements, *J. Appl. Meteorol., 13,* 488–493, 1974.

Marmorino, G. O., and D. R. Caldwell, Horizontal variation of vertical temperature gradients measured by thermocouple arrays, *Deep Sea Res, 25,* 195–181, 1978*a*.

Marmorino, G. O., and D. R. Caldwell, Temperature fine structure and microstructure observations in a coastal upwelling region during a period of variable winds, *Deep Sea Res, 25,* 1073–1106, 1978*b*.

Nasmyth, P. W., Oceanic turbulence, Ph.D. thesis, 69 pp., Inst. of Oceanogr., Univ. of B. C., Vancouver, 1970.

Osborn, T. R., Vertical profiling of velocity microstructure, *J. Phys. Oceanogr., 4,* 109–115, 1974.

Osborn, T. R., and C. S. Cox, Oceanic fine structure, *Geophys. Fluid Dyn., 3,* 321–345, 1972.

Weinstock, J., Vertical turbulent diffusion in a stably stratified fluid, *J. Atmos. Sci., 35,* 1022–1027, 1978.

Williams, R. M., and C. A. Paulson, Microscale temperature and velocity spectra in the atmospheric boundary layer, *J. Fluid Mech., 83,* 547–567, 1977.

(Received April 17, 1979;
revised November 5, 1979;
accepted November 15, 1979.)